

Investigation of phase transformations in a two-layer Ti–Al–C+Y–Al–O coating on a heat-resistant nickel alloy

© 2023

*Almaz Yu. Nazarov**^{1,4}, PhD (Engineering),
assistant professor of Chair of Mechanical Engineering
Aleksey A. Maslov^{1,5}, laboratory assistant of Chair of Mechanical Engineering
*Aleksey A. Nikolaev*¹, assistant of Chair of Mechanical Engineering
Aleksandr N. Shmakov^{2,3}, leading researcher
*Vladimir V. Denisov*³, PhD (Engineering),
Head of Laboratory of Beam-Plasma Surface Engineering
*Kamil N. Ramazanov*¹, Doctor of Sciences (Engineering),
Head of Chair of Mechanical Engineering

¹Ufa University of Science and Technology, Ufa (Russia)

²Federal Research Center Boreskov Institute of Catalysis SB of RAS, Novosibirsk (Russia)

³Institute of High Current Electronics SB of RAS, Tomsk (Russia)

*E-mail: nazarov_almaz15@mail.ru,
nazarov.ayu@ugatu.su

⁴ORCID: <https://orcid.org/0000-0002-4711-4721>

⁵ORCID: <https://orcid.org/0000-0002-2568-1784>

Received 03.07.2023

Accepted 17.11.2023

Abstract: Currently, an active increase in requirements for fuel efficiency and specific gravity of aircraft turbojet engines is observed. Existing coatings based on zirconium dioxide intended for protecting engine parts are largely outdated and have exhausted their development potential, so new ceramic systems for the production of protective coatings based on them are an area of research. The authors carried out a study of a heat-resistant two-layer coating based on the Y–Al–O system (outer layer) and the Ti₂AlC MAX phase of the Ti–Al–C system (sublayer) produced using vacuum-arc deposition on the Inconel 738 heat-resistant nickel alloy and molybdenum by alternate deposition of layers based on Ti–Al–C and a Y–Al–O layer. Using synchrotron radiation, phase transformations in the coating were examined when samples were heated to 1400 °C in a vacuum and to 1100 °C in the atmosphere to study the process of oxidation and coating formation in the presence of oxygen. Using scanning electron microscopy, the authors studied the microstructure and chemical composition of the coating. The study identified that heating the coating in a vacuum and in the atmosphere causes various phase transformations in it, but in both cases, the formation of a mixture of oxides of the Y–Al–O group and destabilization of the Ti–Al–C-based sublayer are observed. After heating the coating in the atmosphere without preliminary heat treatment, the coating was destroyed upon cooling, which was not observed when the coating was heated in a vacuum.

Keywords: heat-resistant coating; ceramic coating; MAX phase; yttrium oxide; vacuum-arc deposition; synchrotron radiation.

Acknowledgments: The work was financially supported by the Ministry of Science and Higher Education of the Russian Federation (Project No. 075-15-2021-1348).

The paper was written on the reports of the participants of the XI International School of Physical Materials Science (SPM-2023), Togliatti, September 11–15, 2023.

For citation: Nazarov A.Yu., Maslov A.A., Nikolaev A.A., Shmakov A.N., Denisov V.V., Ramazanov K.N. Investigation of phase transformations in a two-layer Ti–Al–C+Y–Al–O coating on a heat-resistant nickel alloy. *Frontier Materials & Technologies*, 2023, no. 4, pp. 63–71. DOI: 10.18323/2782-4039-2023-4-66-6.

INTRODUCTION

In modern aircraft engine building, there is a constant search for ways to improve the efficiency of gas turbine engines, due to the growing requirements of aviation regulators. It is known that to improve the efficiency and specific power of engines, the main task is to increase the operating temperature in the combustion chamber, and turbine, which leads to increased requirements for the materials used. Nickel alloys traditionally used in turbines are capable of operating at temperatures up to 1050 °C at the alloy surface; however, this is not enough to operate in modern engines. Therefore, to protect the blades of gas turbine engines, industry applies multilayer heat-barrier and heat-resistant coatings consisting of a sublayer based on

MeCrAlY or the Ni–Al–Pt system, and an external columnar thermal barrier layer based on zirconium dioxide, stabilised with ZrO₂·Y₂O₃ (6...8 wt. %) yttrium oxide. The sublayer based on MeCrAlY, or the Ni–Al–Pt system during operation creates an oxide film layer that prevents oxygen diffusion to the substrate material [1–3]. This protective coating architecture allows the blades to operate at ambient temperatures up to 1300 °C by creating a temperature gradient, between the layer surface and the inner part of the cooled blade [4–6]. However, the mentioned combination of coatings is rapidly becoming obsolete, and is not suitable for the next generation of gas turbine engines, whose operating temperature exceeds 1500 °C in the turbine [7–9]. The reasons for such obsolescence, were the phase transformations occurring in the ceramic layer

at temperatures above 1300 °C on the coating surface, the ceramic layer sintering, a sharp increase in thermal conductivity, and degradation of the heat-resistant sublayer. This leads to the impossibility of further increasing the operating temperature of gas turbine engines without a catastrophic drop in the service life of the blades [10–12].

The listed factors actualise the search for new heat-resistant and heat-barrier coatings to protect the engine blades of the next generations. One of the promising candidates for replacing the traditional ZrO₂–Y₂O₃ coating is the Y–Al–O system including stable Y₃Al₅O₁₂, YAlO₃ and Y₄Al₂O₉ compounds, which demonstrate promising high-temperature characteristics, such as oxidation resistance, and a relatively high thermal expansion coefficient [13–15]. One of the promising candidates for replacing the MCrAlY (Ni–Al–Pt) sublayer can be a coating consisting of the M_{n+1}AX_n phase of Ti₂AlC. The M_{n+1}AX_n phase of Ti₂AlC has high heat resistance due to the formation of a strong α-Al₂O₃ oxide film, and a relatively high thermal expansion coefficient, that allows creating a transition oxidation-resistant sublayer under the Y–Al–O ceramic coating [16–18].

Another important task is the study of the structure and phase transformations in a combined coating, during heating to understand the processes occurring in the coating.

The purpose of this work is to study structural and phase transformations, in a combined Y–Al–O+Ti–Al–C coating when heating the sample in a vacuum, to a temperature of 1400 °C in real time using synchrotron radiation.

METHODS

The coatings of the Ti–Al–C system and the Y–Al–O system were deposited using a modernised NNV-6.6-II installation. The coating was applied to the Inconel 738 alloy and commercially pure (99.96 %) molybdenum. To study the qualitative phase composition, and phase transformations in the coating in real time, when heating the sample to 1400 and 1100 °C, the authors used the following equipment: VEPP-3 synchrotron radiation source of the Institute of Nuclear Physics of the Siberian Branch of the Russian Academy of Sciences, an Anton Paar HTK-2000 high-temperature X-ray camera, OD-3M-350 position-sensitive single-axis detector, and Origin software for data processing.

Due to the peculiarities of the imaging technique using synchrotron radiation with heating in the atmosphere, the maximum test temperature was limited and amounted to 1100 °C. All diffraction patterns are presented in the angle scale corresponding to CuKα radiation (0.15406 nm). To estimate the quantitative content of phases, a method of shooting without a standard was used, based on assessing the ratio of the intensity of the desired phase reflexes to the total intensity of oxide reflexes in the diffraction pattern. The coating structure was studied using a JEOL JSM-6390 scanning electron microscope. Secondary electron mode was used to obtain images of the polished section surface. The coating chemical composition was assessed using the INCA Energy system for energy dispersive microanalysis.

The Ti–Al–C coating was applied by the vacuum-arc method, assisted by a plasma source with an incandescent cathode, through which a mixture of acetylene and argon was supplied in a ratio of 1:4. The discharge current was 10 A. The current on the arc evaporators was 50 and 80 A for titanium and aluminium, respectively, the pressure

in the chamber was 0.3 Pa. Coating deposition time was 2 h. After coating deposition, vacuum heat treatment was carried out at a temperature of 800 °C for 2 h.

The Y–Al–O coating was applied using the vacuum-arc method. A mixture of oxygen and argon was supplied to the chamber in a ratio of 54.5 l/h of argon to 42.7 l/h of oxygen. The discharge current was 55 A. The current on the arc evaporators was 60 and 80 A for yttrium and aluminium, respectively, the pressure in the chamber was 0.3 Pa. Coating deposition time was 2 h.

RESULTS

The study of phase transformations in a Ti–Al–C+Y–Al–O coating when heating in a vacuum

Fig. 1 demonstrates a series of X-ray photographs of the process of heating a coated molybdenum sample in a vacuum, in the form of a projection of the intensity of reflexes, onto the “diffraction angle – temperature” plane. The first frames show that in the initial state, the coating is an amorphous structure – the X-ray diffraction pattern shows a smooth increase in the diffracted intensity, with a maximum in the region of angles of 2θ ~29...31°. Individual reflexes belonging to yttrium and aluminium are recorded. No reflexes of titanium or phases containing titanium and carbon are observed in the diffraction pattern of the initial sample (before heating).

When the sample is heated in a vacuum to 1400 °C, a series of X-ray diffraction patterns shows a change in the phase composition of the coating, which begins at a temperature of ~1200 °C. The amorphous component disappears, and predominantly phases of YAlO₃ mixed oxide and Y₂O₃ yttrium oxide appear. Reflexes related to phases containing titanium or carbon are still not observed. There are no further changes in the coating phase composition when keeping the sample at a temperature of 1400 °C. Fig. 2 presents the final diffraction pattern of a sample with a Ti–Al–C+Y–Al–O coating on molybdenum after cooling to room temperature.

The study of phase transformations in a Ti–Al–C+Y–Al–O coating when heating in the atmosphere

Fig. 3 shows a series of X-ray diffraction patterns of the process of heating a coated Inconel 738 alloy sample in the atmosphere in the form of a projection of the reflex intensity onto the “diffraction angle – temperature” plane. The first frames show that in the initial state, the coating has an amorphous structure with separate yttrium and aluminium reflexes. During heating at a temperature of ~890...910 °C, the broad maximum associated with the amorphous component begins to disappear, and reflexes begin to appear. Their identity is difficult to be accurately determined due to thermal expansion. At the same time, the reflexes of the Y₂O₃, YAlO₃ and Y₄Al₂O₉ oxides appear. Reflexes related to titanium or carbon-containing phases are still not observed. With further exposure of the sample at a temperature of 1100 °C for 1 h, the coating phase composition practically does not change, except for the disappearance of reflexes of aluminium and phase transformations, at the beginning of exposure, which is associated with the diffusion processes, and the formation of oxides in the coating. When cooling the sample after exposure, at

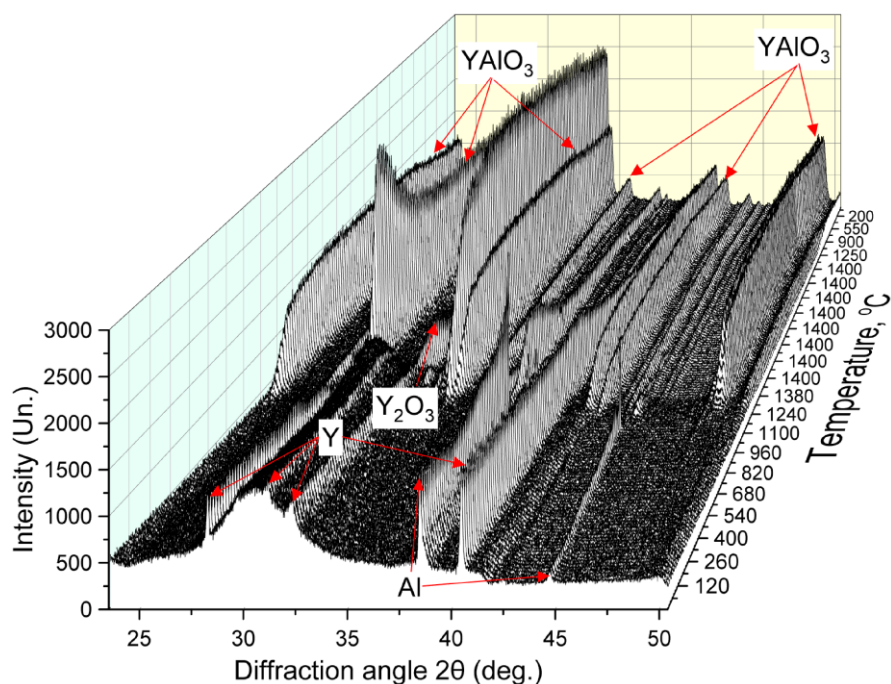


Fig. 1. Series of diffraction patterns of the process of heating a sample with a combined Ti–Al–C+Y–Al–O coating on molybdenum in a vacuum in the form of a set of reflexes in the “diffraction angle – intensity – temperature” coordinates
Рис. 1. Серия дифрактограмм процесса нагрева образца с комбинированным покрытием Ti–Al–C+Y–Al–O на молибдене в вакууме в виде набора рефлексов в координатах «угол дифракции – интенсивность – температура»

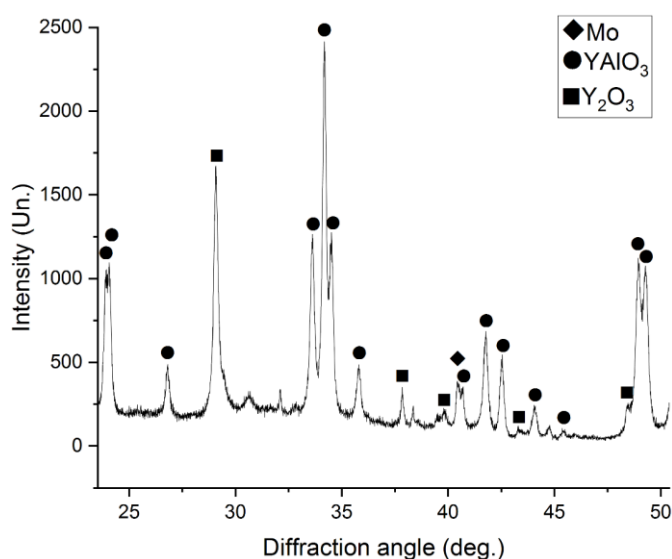


Fig. 2. Diffraction pattern of a sample with a combined Ti–Al–C+Y–Al–O coating on molybdenum after heating and cooling in a vacuum
Рис. 2. Дифрактограмма образца с комбинированным покрытием Ti–Al–C+Y–Al–O на молибдене после прогрева и остывания в вакууме

a temperature of ~ 420 °C, partial coating destruction and peeling occurs, as well as a change in the optical scheme of the experiment, so the final coating composition could not be determined with sufficient accuracy. Therefore, the belonging of reflexes indicated in Fig. 3 and 4 is a matter of judgment. Unlike the previous heating experiment, a complex $Y_4Al_2O_9$ oxide with a monoclinic structure was formed in

this coating. The high intensity of chromium reflexes present in the Inconel 738 alloy is worth noting. The appearance of chromium reflexes indicates a loss of coating continuity and beam penetration to the substrate layer.

Fig. 4 shows the final diffraction pattern of a sample coated with Ti–Al–C+Y–Al–O on the Inconel 738 alloy after cooling to room temperature.

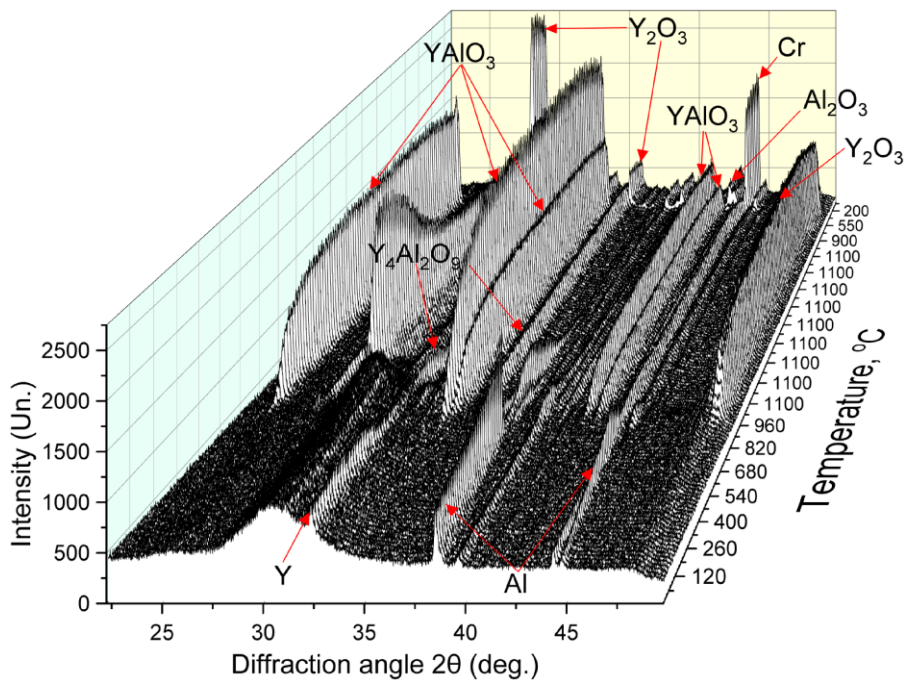


Fig. 3. Series of diffraction patterns of the process of heating a sample with a combined Ti–Al–C+Y–Al–O coating on the Inconel 738 alloy in the atmosphere in the form of a set of reflexes in the “diffraction angle – intensity – temperature” coordinates
Рис. 3. Серия дифрактограмм процесса нагрева образца с комбинированным покрытием Ti–Al–C+Y–Al–O на сплаве Inconel 738 в атмосфере в виде набора рефлексов в координатах «угол дифракции – интенсивность – температура»

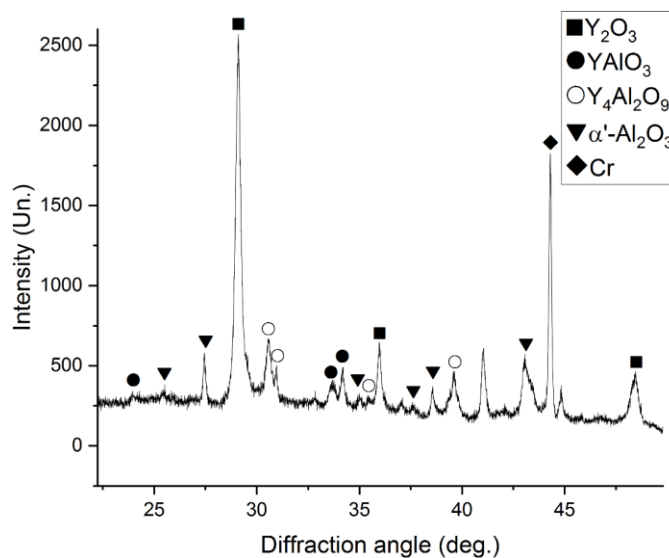


Fig. 4. Diffraction pattern of a sample with a combined Ti–Al–C+Y–Al–O coating on the Inconel 738 alloy after heating and cooling in the atmosphere
Рис. 4. Дифрактограмма образца с комбинированным покрытием Ti–Al–C+Y–Al–O на сплаве Inconel 738 после прогрева и остывания в атмосфере

The study of the coating structure and chemical composition

Fig. 5 and 6 present the results of scanning electron microscopy of samples, with a Ti–Al–C+Y–Al–O coating deposited on the Inconel 738 alloy. Analysis of the images shows the formation of 2 regions: on the outer surface of

the sample there is a Y–Al–O coating, demonstrating a rather non-continuous layered structure (without vacuum heat treatment), underneath there is a Ti–Al–C sublayer (subjected to vacuum heat treatment), which retains its continuity and adhesion to the surface. In the Ti–Al–C layer, an increased nickel content is observed (up to 57 wt. %).

No diffusion is observed between the Y–Al–O and Ti–Al–C layers. Under the coating, two characteristic diffusion zones saturated with aluminium are observed in the alloy.

Table 1 presents a set of points for spectral elemental analysis of coatings. Diffusion zone I (Fig. 5) is located from the boundary of the Ti–Al–C coating deep into the nickel alloy, and has a thickness of $\sim 11 \mu\text{m}$. According to elemental analysis, the zone covered by spectra 9 and 11 consists of intermetallic compounds of the Ni–Al system (spectra 9–11 in Fig. 6 and in Table 1) and possibly contains the δ -phase of the Ni_2Al_3 intermetallic compound, which is stoichiometrically appropriate. This zone also contains an increased content of chromium, which is released along the δ -phase boundaries in the form of finely dispersed particles less than $1 \mu\text{m}$ in size. Diffusion zone II (Fig. 5) is located under diffusion zone I, and has a thickness of $7 \mu\text{m}$. The structure of this zone is characterized by needle-like precipitates of excess phases based on chromium and cobalt.

DISCUSSION

The presented results showed that immediately after deposition, the Y–Al–O coating has an amorphous structure, which was also observed in the works of other authors [15; 21]. To crystallise the YAlO_3 phase, it is necessary to exceed a certain energy level, and maintain the required temperature. Moreover, the cooling rate must be low enough to complete the rearrangement of atoms, and the formation of long-range order [15]. Such conditions can be implemented under conditions of vacuum-arc coating deposition using additional heating sources. However, in this case, due to the non-stationary conditions of deposition at each point of the vacuum chamber, and the sputtering of more low-melting elements during additional heating,

a shift from the stoichiometrically required phase composition and the formation of secondary phases will occur. Therefore, to form the required phase composition, it is rational to carry out subsequent heat treatment of the coating.

The results of studying changes in the phase composition, during vacuum heating of the Y–Al–O coating (Fig. 1), showed that for its complete crystallisation and decomposition of secondary phases, the required annealing temperature is 1200°C . In this case, the coating phase composition will be represented predominantly by the required YAlO_3 phase with a small content of the Y_2O_3 phase. Semi-quantitative analysis based on assessing the ratio of the intensity of the YAlO_3 phase reflexes to the total intensity of all oxide reflexes of the diffraction pattern (Fig. 2), showed that the content of the required phase in the coating is $\sim 85\%$. The formation of the Y_2O_3 phase is caused by the high yttrium content in the coating – up to 60 wt. % (Table 1, spectra 1–5). It follows from this that to form a homogeneous YAlO_3 coating, it is necessary to increase the aluminium component content.

In the work [22], it was noted that the Y_2O_3 phase increases the coating adhesion and has a thermal expansion coefficient similar to the YAlO_3 and Al_2O_3 phases. When the coating is heated in air (Fig. 3), coating crystallisation occurs at lower temperatures. The formation of oxide phases occurs already at a temperature of 890°C . Presumably, this is related to the fact that due to the excess concentration of oxygen from the atmosphere, the surface oxidation occurs, and specified reflexes represent the phase composition of the surface layer, and not the coating as a whole. In this case, during the cooling process, coating peeling occurred, which is associated with stresses and cracks that appeared immediately after deposition (Fig. 5), as well as with a high oxidation rate compared to vacuum heating. The formation

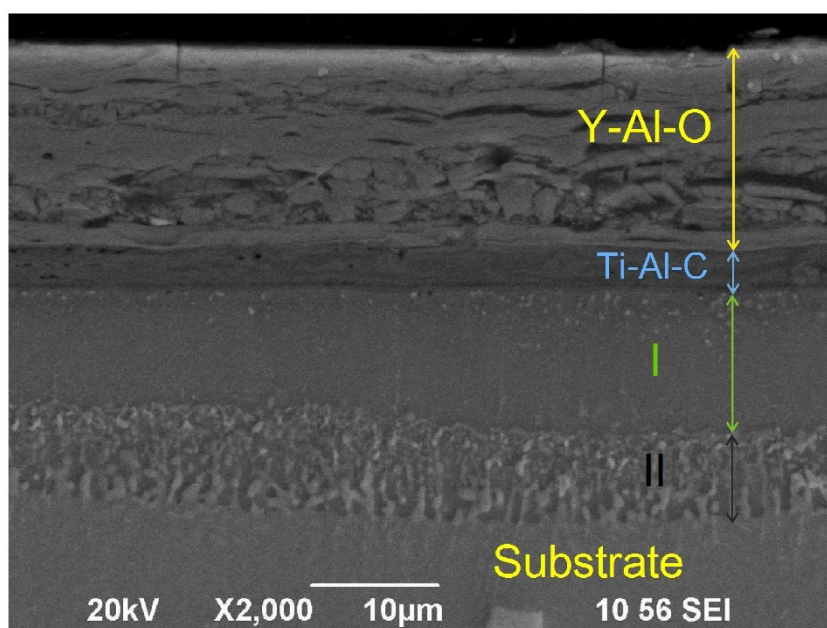


Fig. 5. The structure of the combined Y–Al–O+Ti–Al–C coating on the Inconel 738 alloy after deposition
Рис. 5. Структура комбинированного покрытия Y–Al–O+Ti–Al–C на сплаве Inconel 738 после осаждения

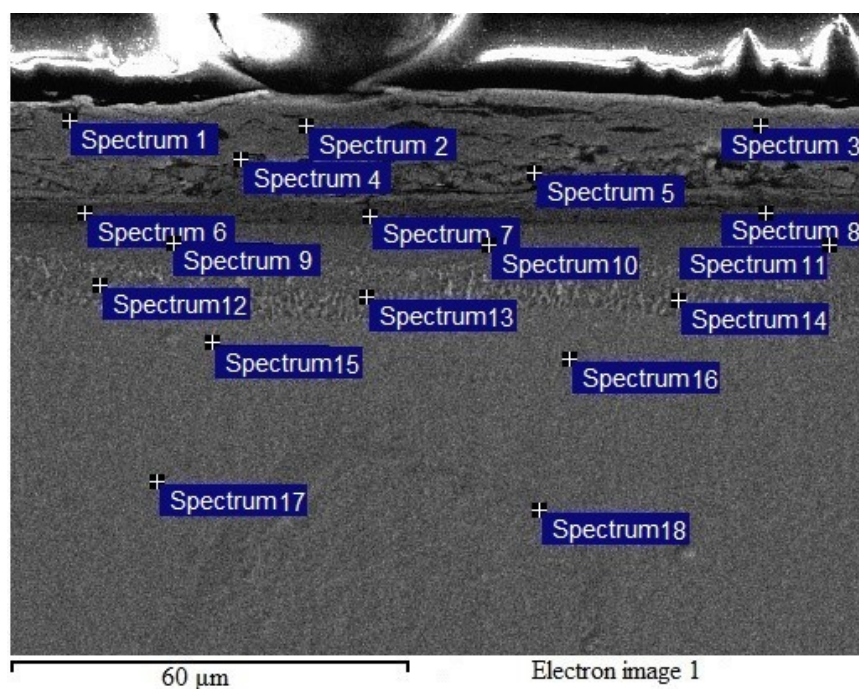


Fig. 6. Set of points for spectral analysis
Рис. 6. Набор точек для спектрального анализа

Table 1. Results of spectral analysis by points
Таблица 1. Результаты спектрального анализа по точкам

Spectrum	O	Al	Ti	Cr	Co	Ni	Y
Spectrum 1	22.34	17.67	0.00	0.00	0.00	0.00	59.99
Spectrum 2	26.01	16.05	0.00	0.00	0.00	0.00	57.95
Spectrum 3	25.25	16.28	0.00	0.36	0.00	0.00	58.11
Spectrum 4	20.84	20.13	0.33	0.00	0.00	0.00	58.70
Spectrum 5	17.77	29.22	5.72	0.00	0.00	1.95	45.34
Spectrum 6	7.17	16.04	51.39	1.60	2.19	21.61	0.00
Spectrum 7	0.00	24.48	6.99	4.36	6.68	57.49	0.00
Spectrum 8	0.00	26.30	16.73	2.88	4.92	49.18	0.00
Spectrum 9	0.00	20.64	4.11	6.00	7.32	61.93	0.00
Spectrum 10	3.53	11.13	4.33	36.93	6.48	37.61	0.00
Spectrum 11	0.00	19.99	4.96	7.23	7.83	59.99	0.00
Spectrum 12	0.00	14.08	4.87	10.92	9.44	60.68	0.00
Spectrum 13	4.29	9.53	4.20	22.24	10.36	49.39	0.00
Spectrum 14	0.00	6.10	5.72	16.24	9.12	62.82	0.00
Spectrum 15	2.83	3.74	3.19	19.74	10.37	60.12	0.00
Spectrum 16	0.00	5.08	3.75	15.54	7.78	67.86	0.00
Spectrum 17	0.00	2.60	2.89	23.18	11.49	59.85	0.00
Spectrum 18	3.54	2.50	2.11	22.20	10.87	58.77	0.00

of cracks is apparently caused by the occurrence of unwanted stresses in the coating due to the discrepancy between the physical and mechanical properties of the Ti₂AlC phase and the Y–Al–O layer. For an exact explanation, additional study and determination of the optimal parameters for the Y–Al–O coating deposition are required.

CONCLUSIONS

In this work, using synchrotron radiation, the authors studied real-time phase transformations in a two-layer Ti–Al–C+Y–Al–O coating. During heating in a vacuum to a temperature of 1400 °C, the coating crystallises with the formation of predominantly YAlO₃ yttrium orthoaluminate and Y₂O₃ yttrium oxide. After heating in the atmosphere, the coating crystallises with the formation of a mixture of YAlO₃, Y₂O₃, and Y₄Al₂O₉ oxides; however, if heated in the atmosphere, the coating is destroyed upon cooling.

REFERENCES

- Mondal K., Nunez L., Lii C.M., Downey I.J., Rooyen I.J. Thermal barrier coatings overview: Design, manufacturing, and applications in high-temperature industries. *Industrial & Engineering Chemistry Research*, 2021, vol. 60, no. 17, pp. 6061–6077. DOI: [10.1021/acs.iecr.1c00788](https://doi.org/10.1021/acs.iecr.1c00788).
- Liu Bin, Liu Yuchen, Zhu Changhua, Xiang Huimin, Chen Hongfei, Sun Luchao, Gao Yanfeng, Zhou Yanchun. Advances on strategies for searching for next generation thermal barrier coating materials. *Journal of Materials Science & Technology*, 2019, vol. 35, no. 5, pp. 833–851. DOI: [10.1016/j.jmst.2018.11.016](https://doi.org/10.1016/j.jmst.2018.11.016).
- Vaßen R., Bakan E., Mack D.E., Guillon O. A perspective on thermally sprayed thermal barrier coatings: current status and trends. *Journal of Thermal Spray Technology*, 2022, vol. 31, no. 4, pp. 685–698. DOI: [10.1007/s11666-022-01330-2](https://doi.org/10.1007/s11666-022-01330-2).
- Lashmi P.G., Ananthapadmanabhan P.V., Unnikrishnan G., Aruna S.T. Present status and future prospects of plasma sprayed multilayered thermal barrier coating systems. *Journal of the European Ceramic Society*, 2020, vol. 40, no. 8, pp. 2731–2745. DOI: [10.1016/j.jeurceramsoc.2020.03.016](https://doi.org/10.1016/j.jeurceramsoc.2020.03.016).
- Thakare J.G., Pandey Ch., Mahapatra M.M., Mulik R.S. Thermal barrier coatings – A state of the art review. *Metals and Materials International*, 2021, vol. 27, pp. 1947–1968. DOI: [10.1007/s12540-020-00705-w](https://doi.org/10.1007/s12540-020-00705-w).
- Cernuschi F., Bison P. Thirty Years of Thermal Barrier Coatings (TBC), Photothermal and thermographic techniques: Best practices and lessons learned. *Journal of Thermal Spray Technology*, 2022, vol. 31, no. 4, pp. 716–744. DOI: [10.1007/s11666-022-01344-w](https://doi.org/10.1007/s11666-022-01344-w).
- Tejero-Martin D., Bennett C., Hussain T. A review on environmental barrier coatings: History, current state of the art and future developments. *Journal of the European Ceramic Society*, 2021, vol. 41, no. 3, pp. 1747–1768. DOI: [10.1016/j.jeurceramsoc.2020.10.057](https://doi.org/10.1016/j.jeurceramsoc.2020.10.057).
- Liu Yuchen, Zhang Wei, Wang Banghui, Sun Luchao, Li Fangzhi, Xue Zhenhai, Zhou Guohong, Liu Bin, Nian Hanggiang. Theoretical and experimental investigations on high temperature mechanical and thermal properties of BaZrO₃. *Ceramics International*, 2018, vol. 44, no. 14, pp. 16475–16482. DOI: [10.1016/j.ceramint.2018.06.064](https://doi.org/10.1016/j.ceramint.2018.06.064).
- Jarligo M.O., Mack D.E., Vassen R., Stover D. Application of plasma-sprayed complex perovskites as thermal barrier coatings. *Journal of Thermal Spray Technology*, 2009, vol. 18, pp. 187–193. DOI: [10.1007/s11666-009-9302-9](https://doi.org/10.1007/s11666-009-9302-9).
- Guo Hongbo, Zhang Hongju, Ma Guohui, Gong Shengkai. Thermo-physical and thermal cycling properties of plasma-sprayed BaLa₂Ti₃O₁₀ coating as potential thermal barrier materials. *Surface and Coatings Technology*, 2009, vol. 204, no. 5, pp. 691–696. DOI: [10.1016/j.surfcoat.2009.09.009](https://doi.org/10.1016/j.surfcoat.2009.09.009).
- Yuan Jieyan, Sun Junbin, Wang Jinshuang, Zhang Hao, Dong Shujuan, Jiang Jianing, Deng Longhui, Zhou Xin, Cao Xueqiang. SrCeO₃ as a novel thermal barrier coating candidate for high-temperature applications. *Journal of Alloys and Compounds*, 2018, vol. 740, pp. 519–528. DOI: [10.1016/j.jallcom.2018.01.021](https://doi.org/10.1016/j.jallcom.2018.01.021).
- Li Enbo, Ma Wen, Zhang Peng, Zhang Chennan, Bai Yu, Liu Hongxia, Yan Shufang, Dong Hongying, Meng Xiangfeng. The effect of Al³⁺ doping on the infrared radiation and thermophysical properties of SrZrO₃ perovskites as potential low thermal infrared material. *Acta Materialia*, 2021, vol. 209, article number 116795. DOI: [10.1016/j.actamat.2021.116795](https://doi.org/10.1016/j.actamat.2021.116795).
- Plaza A.V., Krause A.R. Mitigating CMAS Attack in Model YAlO₃ Environmental Barrier Coatings: Effect of YAlO₃ Crystal Orientation on Apatite Nucleation. *Coatings*, 2022, vol. 12, no. 10, article number 1604. DOI: [10.3390/coatings12101604](https://doi.org/10.3390/coatings12101604).
- Turcer L.R., Krause A.R., Garces H.F., Lin Zhang, Padture N.P. Environmental-barrier coating ceramics for resistance against attack by molten calcia-magnesia-aluminosilicate (CMAS) glass: Part I, YAlO₃ and γ-Y₂Si₂O₇. *Journal of the European Ceramic Society*, 2018, vol. 38, no. 11, pp. 3905–3913. DOI: [10.1016/j.jeurceramsoc.2018.03.021](https://doi.org/10.1016/j.jeurceramsoc.2018.03.021).
- Gatzen C., Mack D.E., Guillon O., Vaben R. YAlO₃ – a novel environmental barrier coating for Al₂O₃/Al₂O₃–ceramic matrix composites. *Coatings*, 2019, vol. 9, no. 10, article number 609. DOI: [10.3390/coatings9100609](https://doi.org/10.3390/coatings9100609).
- Haftani M., Heydari M.S., Baharvandi H.R., Ehsani N. Studying the oxidation of Ti₂AlC MAX phase in atmosphere: A review. *International Journal of Refractory Metals and Hard Materials*, 2016, vol. 61, pp. 51–60. DOI: [10.1016/j.jrmhm.2016.07.006](https://doi.org/10.1016/j.jrmhm.2016.07.006).
- Badie S., Sebold D., Vaben R., Guillon O., Gonzalez-Julian J. Mechanism for breakaway oxidation of the Ti₂AlC MAX phase. *Acta Materialia*, 2021, vol. 215, article number 117025. DOI: [10.1016/j.actamat.2021.117025](https://doi.org/10.1016/j.actamat.2021.117025).
- Eklund P., Rosen J., Persson P.O. Layered ternary M_{n+1}AX_n phases and their 2D derivative MXene: an overview from a thin-film perspective. *Journal of Physics D: Applied Physics*, 2017, vol. 50, no. 11, article number 113001. DOI: [10.1088/1361-6463/aa57bc](https://doi.org/10.1088/1361-6463/aa57bc).
- Garkas W., Leyens C., Flores-Renteria A. Synthesis and characterization of Ti₂AlC and Ti₂AlN MAX phase coatings manufactured in an industrial-size coater.

- Advanced Materials Research*, 2010, vol. 89, pp. 208–213. DOI: [10.4028/www.scientific.net/AMR.89-91.208](https://doi.org/10.4028/www.scientific.net/AMR.89-91.208).
20. Tang C., Klimenkov M., Jaentsch U., Leiste H., Rinke M., Ulrich S., Steinbruck M., Saifert H.J., Stueber M. Synthesis and characterization of Ti₂AlC coatings by magnetron sputtering from three elemental targets and ex-situ annealing. *Surface and Coatings Technology*, 2017, vol. 309, pp. 445–455. DOI: [10.1016/j.surfcoat.2016.11.090](https://doi.org/10.1016/j.surfcoat.2016.11.090).
 21. Weyant C.M., Faber K.T. Processing–microstructure relationships for plasma-sprayed yttrium aluminum garnet. *Surface and Coatings Technology*, 2008, vol. 202, no. 24, pp. 6081–6089. DOI: [10.1016/j.surfcoat.2008.07.008](https://doi.org/10.1016/j.surfcoat.2008.07.008).
 22. Mechnich P., Braue W. Air plasma-sprayed Y₂O₃ coatings for Al₂O₃/Al₂O₃ ceramic matrix composites. *Journal of the European Ceramic Society*, 2013, vol. 33, no. 13-14, pp. 2645–2653. DOI: [10.1016/j.jeurceramsoc.2013.03.034](https://doi.org/10.1016/j.jeurceramsoc.2013.03.034).
- ### СПИСОК ЛИТЕРАТУРЫ
1. Mondal K., Nunez L., Lii C.M., Downey I.J., Rooyen I.J. Thermal barrier coatings overview: Design, manufacturing, and applications in high-temperature industries // *Industrial & Engineering Chemistry Research*. 2021. Vol. 60. № 17. P. 6061–6077. DOI: [10.1021/acs.iecr.1c00788](https://doi.org/10.1021/acs.iecr.1c00788).
 2. Liu Bin, Liu Yuchen, Zhu Changhua, Xiang Huimin, Chen Hongfei, Sun Luchao, Gao Yanfeng, Zhou Yanchun. Advances on strategies for searching for next generation thermal barrier coating materials // *Journal of Materials Science & Technology*. 2019. Vol. 35. № 5. P. 833–851. DOI: [10.1016/j.jmst.2018.11.016](https://doi.org/10.1016/j.jmst.2018.11.016).
 3. Vaßen R., Bakan E., Mack D.E., Guillon O. A perspective on thermally sprayed thermal barrier coatings: current status and trends // *Journal of Thermal Spray Technology*. 2022. Vol. 31. № 4. P. 685–698. DOI: [10.1007/s11666-022-01330-2](https://doi.org/10.1007/s11666-022-01330-2).
 4. Lashmi P.G., Ananthapadmanabhan P.V., Unnikrishnan G., Aruna S.T. Present status and future prospects of plasma sprayed multilayered thermal barrier coating systems // *Journal of the European Ceramic Society*. 2020. Vol. 40. № 8. P. 2731–2745. DOI: [10.1016/j.jeurceramsoc.2020.03.016](https://doi.org/10.1016/j.jeurceramsoc.2020.03.016).
 5. Thakare J.G., Pandey Ch., Mahapatra M.M., Mulik R.S. Thermal barrier coatings – A state of the art review // *Metals and Materials International*. 2021. Vol. 27. P. 1947–1968. DOI: [10.1007/s12540-020-00705-w](https://doi.org/10.1007/s12540-020-00705-w).
 6. Cernuschi F., Bison P. Thirty Years of Thermal Barrier Coatings (TBC), Photothermal and thermographic techniques: Best practices and lessons learned // *Journal of Thermal Spray Technology*. 2022. Vol. 31. № 4. P. 716–744. DOI: [10.1007/s11666-022-01344-w](https://doi.org/10.1007/s11666-022-01344-w).
 7. Tejero-Martin D., Bennett C., Hussain T. A review on environmental barrier coatings: History, current state of the art and future developments // *Journal of the European Ceramic Society*. 2021. Vol. 41. № 3. P. 1747–1768. DOI: [10.1016/j.jeurceramsoc.2020.10.057](https://doi.org/10.1016/j.jeurceramsoc.2020.10.057).
 8. Liu Yuchen, Zhang Wei, Wang Banghui, Sun Luchao, Li Fangzhi, Xue Zhenhai, Zhou Guohong, Liu Bin, Nian Hanggiang. Theoretical and experimental investigations on high temperature mechanical and thermal properties of BaZrO₃ // *Ceramics International*. 2018. Vol. 44. № 14. P. 16475–16482. DOI: [10.1016/j.ceramint.2018.06.064](https://doi.org/10.1016/j.ceramint.2018.06.064).
 9. Jarligo M.O., Mack D.E., Vassen R., Stover D. Application of plasma-sprayed complex perovskites as thermal barrier coatings // *Journal of Thermal Spray Technology*. 2009. Vol. 18. P. 187–193. DOI: [10.1007/s11666-009-9302-9](https://doi.org/10.1007/s11666-009-9302-9).
 10. Guo Hongbo, Zhang Hongju, Ma Guohui, Gong Shengkai. Thermo-physical and thermal cycling properties of plasma-sprayed BaLa₂Ti₃O₁₀ coating as potential thermal barrier materials // *Surface and Coatings Technology*. 2009. Vol. 204. № 5. P. 691–696. DOI: [10.1016/j.surfcoat.2009.09.009](https://doi.org/10.1016/j.surfcoat.2009.09.009).
 11. Yuan Jieyan, Sun Junbin, Wang Jinshuang, Zhang Hao, Dong Shujuan, Jiang Jianing, Deng Longhui, Zhou Xin, Cao Xueqiang. SrCeO₃ as a novel thermal barrier coating candidate for high-temperature applications // *Journal of Alloys and Compounds*. 2018. Vol. 740. P. 519–528. DOI: [10.1016/j.jallcom.2018.01.021](https://doi.org/10.1016/j.jallcom.2018.01.021).
 12. Li Enbo, Ma Wen, Zhang Peng, Zhang Chennan, Bai Yu, Liu Hongxia, Yan Shufang, Dong Hongying, Meng Xiangfeng. The effect of Al³⁺ doping on the infrared radiation and thermophysical properties of SrZrO₃ perovskites as potential low thermal infrared material // *Acta Materialia*. 2021. Vol. 209. Article number 116795. DOI: [10.1016/j.actamat.2021.116795](https://doi.org/10.1016/j.actamat.2021.116795).
 13. Plaza A.V., Krause A.R. Mitigating CMAS Attack in Model YAlO₃ Environmental Barrier Coatings: Effect of YAlO₃ Crystal Orientation on Apatite Nucleation // *Coatings*. 2022. Vol. 12. № 10. Article number 1604. DOI: [10.3390/coatings12101604](https://doi.org/10.3390/coatings12101604).
 14. Turcer L.R., Krause A.R., Garces H.F., Lin Zhang, Padture N.P. Environmental-barrier coating ceramics for resistance against attack by molten calcia-magnesia-aluminosilicate (CMAS) glass: Part I, YAlO₃ and γ-Y₂Si₂O₇ // *Journal of the European Ceramic Society*. 2018. Vol. 38. № 11. P. 3905–3913. DOI: [10.1016/j.jeurceramsoc.2018.03.021](https://doi.org/10.1016/j.jeurceramsoc.2018.03.021).
 15. Gatzen C., Mack D.E., Guillon O., Vaben R. YAlO₃ – a novel environmental barrier coating for Al₂O₃/Al₂O₃–ceramic matrix composites // *Coatings*. 2019. Vol. 9. № 10. Article number 609. DOI: [10.3390/coatings9100609](https://doi.org/10.3390/coatings9100609).
 16. Haftani M., Heydari M.S., Baharvandi H.R., Ehsani N. Studying the oxidation of Ti₂AlC MAX phase in atmosphere: A review // *International Journal of Refractory Metals and Hard Materials*. 2016. Vol. 61. P. 51–60. DOI: [10.1016/j.jirmhm.2016.07.006](https://doi.org/10.1016/j.jirmhm.2016.07.006).
 17. Badie S., Sebold D., Vaben R., Guillon O., Gonzalez-Julian J. Mechanism for breakaway oxidation of the Ti₂AlC MAX phase // *Acta Materialia*. 2021. Vol. 215. Article number 117025. DOI: [10.1016/j.actamat.2021.117025](https://doi.org/10.1016/j.actamat.2021.117025).
 18. Eklund P., Rosen J., Persson P.O. Layered ternary M_{n+1}AX_n phases and their 2D derivative MXene: an overview from a thin-film perspective // *Journal of Physics D: Applied Physics*. 2017. Vol. 50. № 11. Article number 113001. DOI: [10.1088/1361-6463/aa57bc](https://doi.org/10.1088/1361-6463/aa57bc).
 19. Garkas W., Leyens C., Flores-Renteria A. Synthesis and characterization of Ti₂AlC and Ti₂AlN MAX phase coatings manufactured in an industrial-size coater // *Advanced Materials Research*. 2010. Vol. 89. P. 208–213. DOI: [10.4028/www.scientific.net/AMR.89-91.208](https://doi.org/10.4028/www.scientific.net/AMR.89-91.208).

20. Tang C., Klimenkov M., Jaentsch U., Leiste H., Rinke M., Ulrich S., Steinbruck M., Saifert H.J., Stueber M. Synthesis and characterization of Ti₂AlC coatings by magnetron sputtering from three elemental targets and ex-situ annealing // *Surface and Coatings Technology*. 2017. Vol. 309. P. 445–455. DOI: [10.1016/j.surfcoat.2016.11.090](https://doi.org/10.1016/j.surfcoat.2016.11.090).
21. Weyant C.M., Faber K.T. Processing–microstructure relationships for plasma-sprayed yttrium aluminum garnet // *Surface and Coatings Technology*. 2008. Vol. 202. № 24. P. 6081–6089. DOI: [10.1016/j.surfcoat.2008.07.008](https://doi.org/10.1016/j.surfcoat.2008.07.008).
22. Mechnich P., Braue W. Air plasma-sprayed Y₂O₃ coatings for Al₂O₃/Al₂O₃ ceramic matrix composites // *Journal of the European Ceramic Society*. 2013. Vol. 33. № 13-14. P. 2645–2653. DOI: [10.1016/j.jeurceramsoc.2013.03.034](https://doi.org/10.1016/j.jeurceramsoc.2013.03.034).

Исследование фазовых превращений в двухслойном жаростойком покрытии Ti–Al–C+Y–Al–O на жаропрочном никелевом сплаве

© 2023

Назаров Алмаз Юнирович^{*1,4}, кандидат технических наук,
доцент кафедры технологии машиностроения
Маслов Алексей Андреевич^{1,5}, лаборант кафедры технологии машиностроения
*Николаев Алексей Александрович*¹, ассистент кафедры технологии машиностроения
Шмаков Александр Николаевич^{2,3}, ведущий научный сотрудник
*Денисов Владимир Викторович*³, кандидат технических наук,
заведующий лабораторией пучково-плазменной инженерии поверхности
*Рамазанов Камиль Нуруллаевич*¹, доктор технических наук,
заведующий кафедрой технологии машиностроения

¹Уфимский университет науки и технологий, Уфа (Россия)

²Федеральный исследовательский центр «Институт катализа им. Г.К. Борескова СО РАН», Новосибирск (Россия)

³Институт сильноточной электроники СО РАН, Томск (Россия)

*E-mail: nazarov_almaz15@mail.ru,
nazarov.ayu@ugatu.su

⁴ORCID: <https://orcid.org/0000-0002-4711-4721>

⁵ORCID: <https://orcid.org/0000-0002-2568-1784>

Поступила в редакцию 03.07.2023

Принята к публикации 17.11.2023

Аннотация: На сегодняшний день происходит активный рост требований к топливной эффективности и удельному весу авиационных турбореактивных двигателей. Существующие покрытия для защиты деталей двигателей на основе диоксида циркония во многом устарели и исчерпали потенциал развития, поэтому ведутся исследования новых керамических систем для производства защитных покрытий на их основе. В работе проведено исследование жаростойкого двухслойного покрытия на основе системы Y–Al–O (внешний слой) и MAX-фазы Ti₂AlC системы Ti–Al–C (подслой), полученного методом вакуумно-дугового осаждения на жаропрочном никелевом сплаве Inconel 738 и на молибдене поочередным осаждением слоев на основе Ti–Al–C и слоя Y–Al–O. При помощи синхротронного излучения исследованы фазовые превращения в покрытии при нагреве образцов до 1400 °C в вакууме и до 1100 °C в атмосфере с целью изучения процесса окисления и формирования покрытия в условиях присутствия кислорода. При помощи растровой электронной микроскопии изучены микроструктура и химический состав покрытия. Установлено, что нагрев покрытия в вакууме и в атмосфере вызывает в нем различные фазовые превращения, но в обоих случаях наблюдается формирование смеси оксидов группы Y–Al–O и дестабилизация подслоя на основе Ti–Al–C. После нагрева покрытия в атмосфере без предварительной термообработки при остывании покрытие разрушилось, чего не наблюдалось при нагреве покрытия в вакууме.

Ключевые слова: жаростойкое покрытие; керамическое покрытие; MAX-фаза; оксид иттрия; вакуумно-дуговое осаждение; синхротронное излучение.

Благодарности: Работа выполнена при финансовой поддержке Министерства науки и высшего образования Российской Федерации (проект № 075-15-2021-1348).

Статья подготовлена по материалам докладов участников XI Международной школы «Физическое материаловедение» (ШФМ-2023), Тольятти, 11–15 сентября 2023 года.

Для цитирования: Назаров А.Ю., Маслов А.А., Николаев А.А., Шмаков А.Н., Денисов В.В., Рамазанов К.Н. Исследование фазовых превращений в двухслойном жаростойком покрытии Ti–Al–C+Y–Al–O на жаропрочном никелевом сплаве // *Frontier Materials & Technologies*. 2023. № 4. С. 63–71. DOI: 10.18323/2782-4039-2023-4-66-6.